



AMS

American Meteorological Society

Supplemental Material

Journal of the Atmospheric Sciences

Variable Rainfall over Steady SST: The Effect of the Free Troposphere on Surface Pressure in
the East Pacific

<https://doi.org/10.1175/JAS-D-23-0101.1>

© [Copyright 2023 American Meteorological Society](#) (AMS)

For permission to reuse any portion of this work, please contact permissions@ametsoc.org. Any use of material in this work that is determined to be “fair use” under Section 107 of the U.S. Copyright Act (17 USC §107) or that satisfies the conditions specified in Section 108 of the U.S. Copyright Act (17 USC §108) does not require AMS’s permission. Republication, systematic reproduction, posting in electronic form, such as on a website or in a searchable database, or other uses of this material, except as exempted by the above statement, requires written permission or a license from AMS. All AMS journals and monograph publications are registered with the Copyright Clearance Center (<https://www.copyright.com>). Additional details are provided in the AMS Copyright Policy statement, available on the AMS website (<https://www.ametsoc.org/PUBSCopyrightPolicy>).

1 **Supplemental Materials for Variable Rainfall over Steady SST: The Effect of**
2 **the Free Troposphere on Surface Pressure in the East Pacific**

3 Isabelle Bunge^a, Adam Sobel^{a,b}, Michela Biasutti^b, Shuguang Wang^c

4 ^a *Columbia University, Department of Applied Physics and Applied Mathematics*

5 ^b *Columbia University, Lamont-Doherty Earth Observatory*

6 ^c *School of Atmospheric Sciences, Nanjing University, Nanjing 210023, China*

7 *Corresponding author: Isabelle Bunge, ieb2123@columbia.edu*

8 **1. Supplemental Figures**

Rainfall Region	Longitudinal Extents
A	[90°W, 86°W]
B	[120°W, 86°W]
C	[160°W, 86°W]

9 Tab. S1. The longitudinal extents for each of the precipitation binning regions applied in the analysis. The
 10 latitude range of each region is set according to the seasonal mean where rainfall is greater than 0.2 mm/hr.

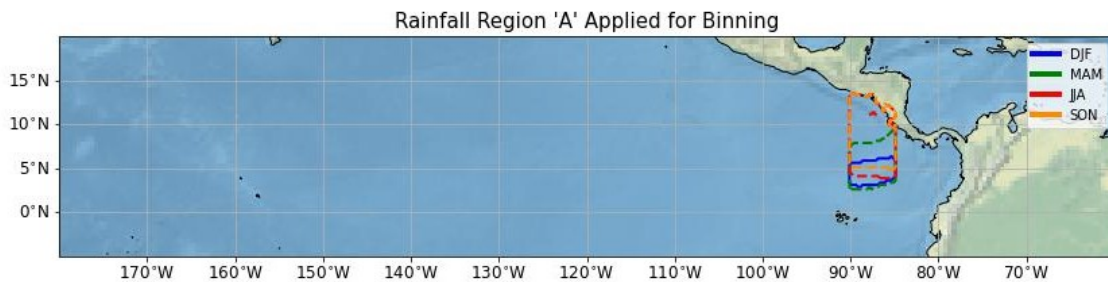


Fig. S1. This figure demonstrates the rainfall region, denoted A, used for precipitation binning.

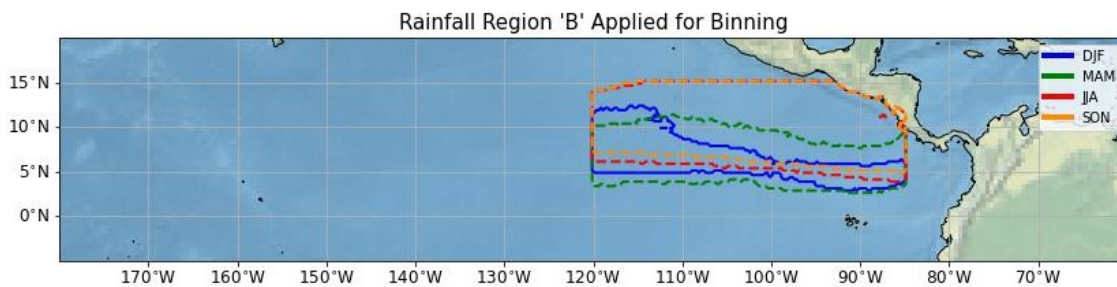
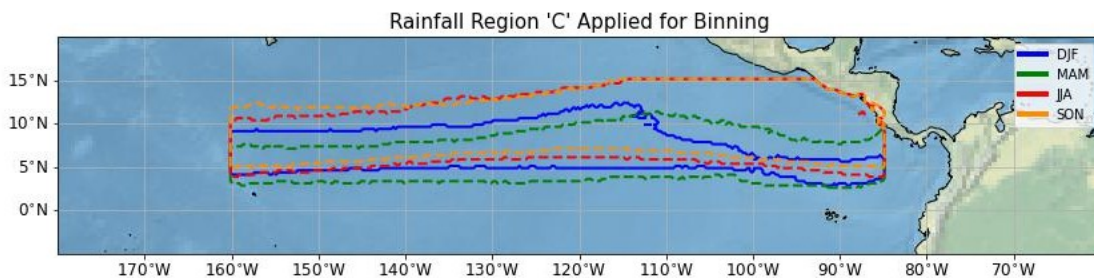
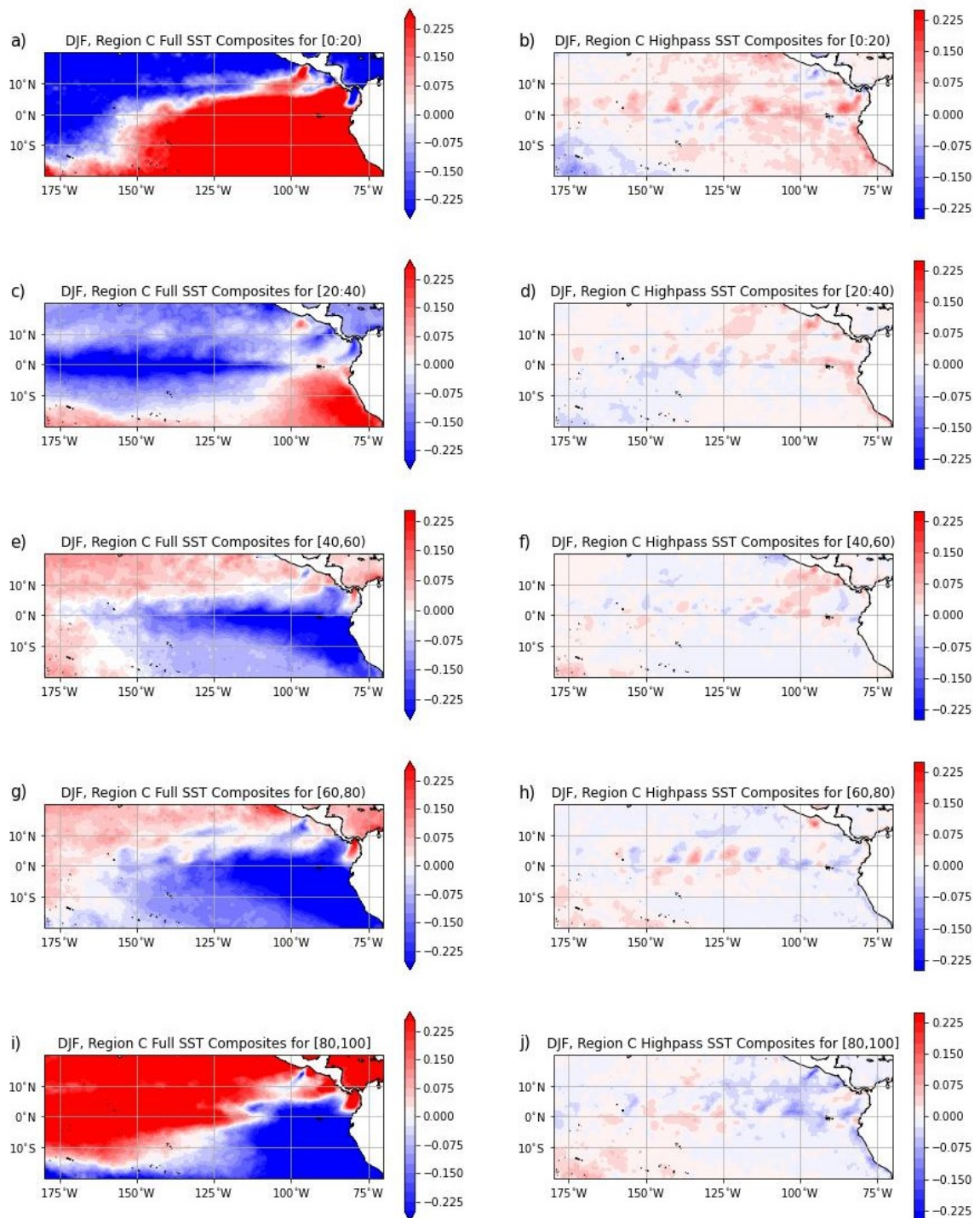


Fig. S2. This figure demonstrates the rainfall region, denoted B, used for precipitation binning.



11 Fig. S3. This figure demonstrates the rainfall region, denoted C, used for precipitation binning. The results
 12 for binning done over region C are presented in the paper.



13 Fig. S4. Figures (a), (c), (e), (g), and (i) show the unfiltered DJF SST composited on each of the rainfall
 14 quintiles. Figures (b), (d), (f), (h), and (j) show the same composites, but for the high-pass filtered DJF SST.

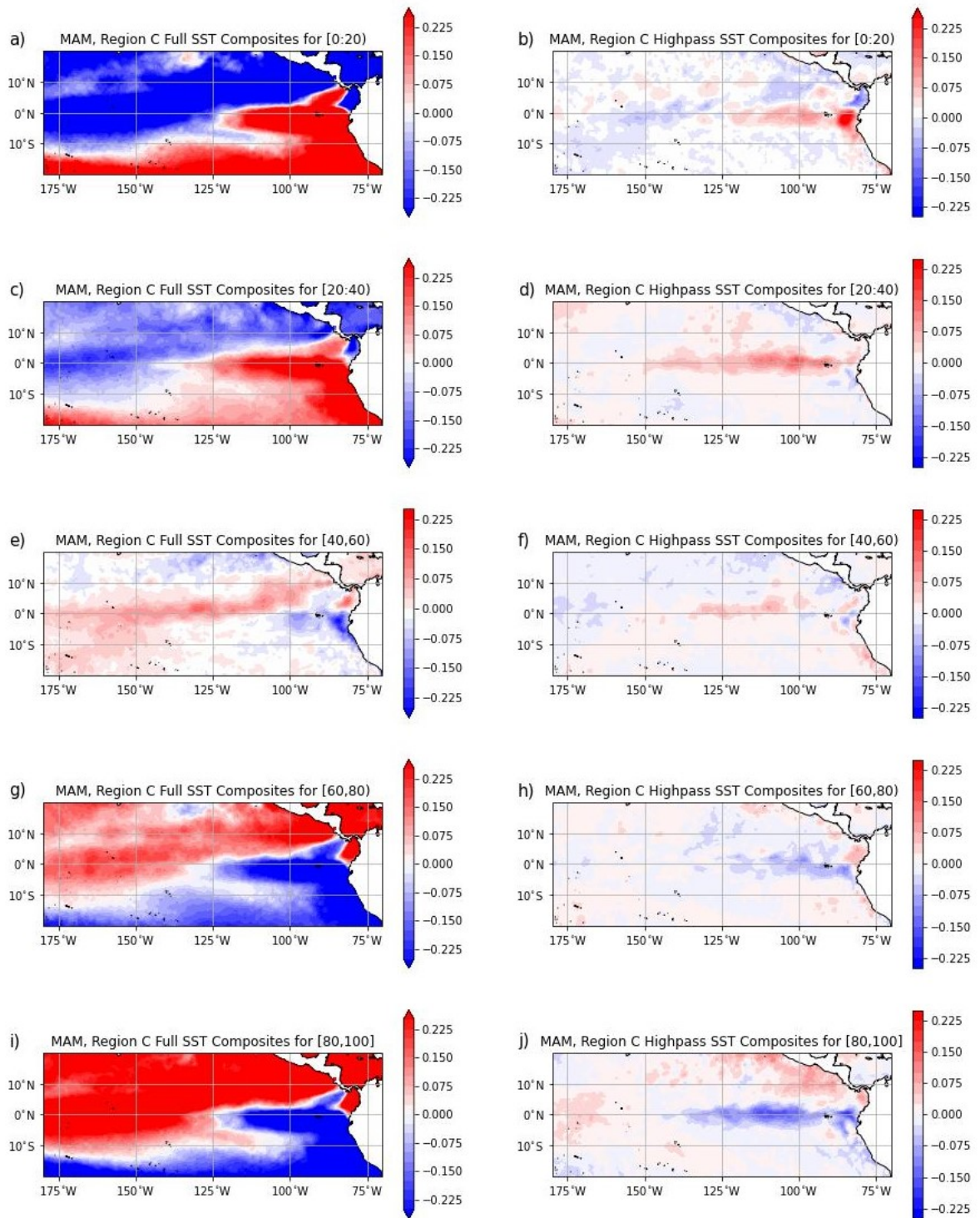


Fig. S5. : Same as Figure S4, but for the unfiltered and high-pass filtered data from MAM

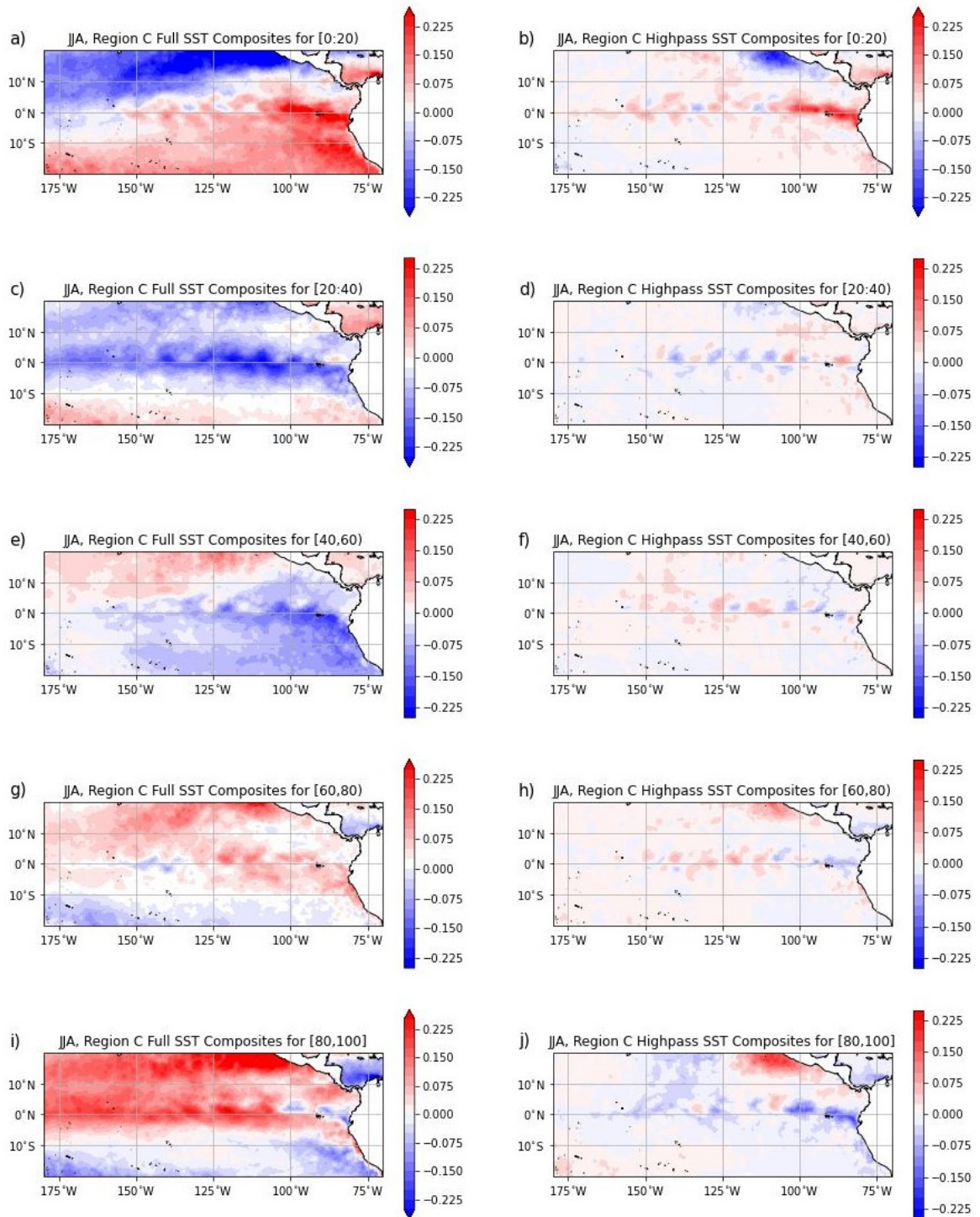


Fig. S6. : Same as Figure S4, but for the unfiltered and high-pass filtered data from JJJA

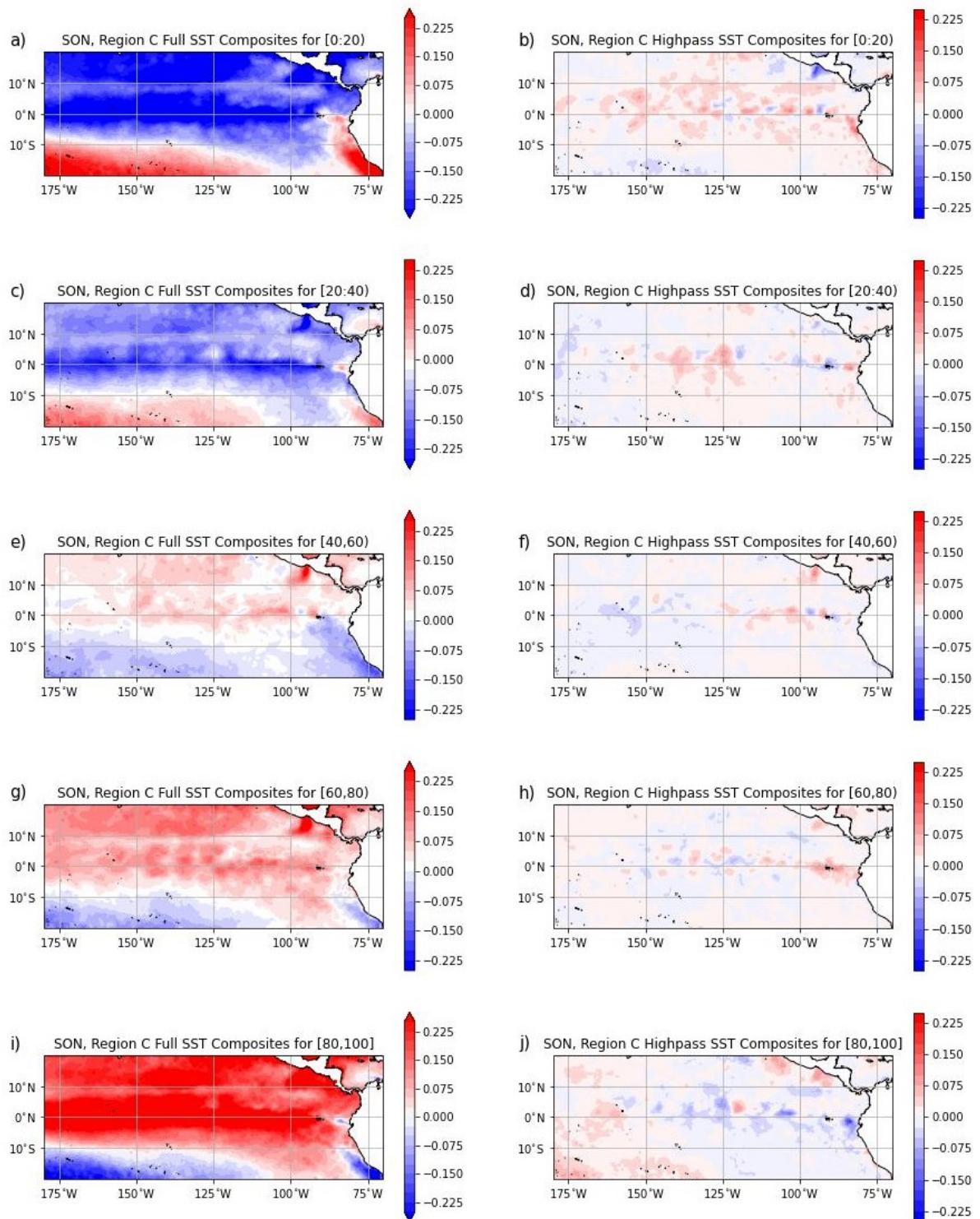
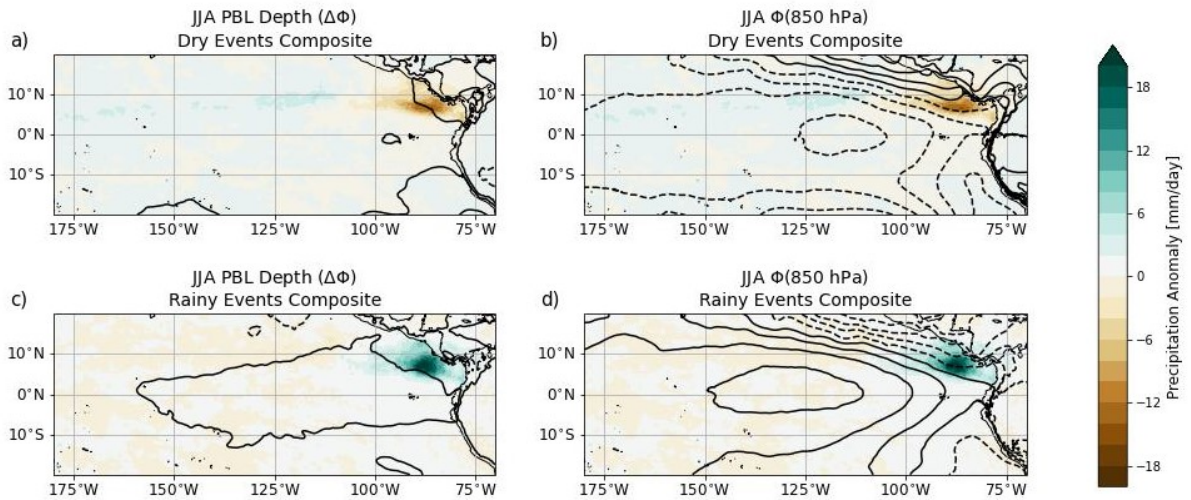


Fig. S7. : Same as Figure S4, but for the unfiltered and high-pass filtered data from SON



15 Fig. S8. The JJA daily geopotential component anomalies composited by daily precipitation quintiles over
 16 region A. Figures (a) and (c) show the PBL depth anomalies for the driest and rainiest quintiles, respectively.
 17 Figures (b) and (d) show the 850 hPa geopotential anomalies for the driest and rainiest quintiles, respectively.
 18 The contour interval for the geopotential anomalies is $10 \text{ m}^2\text{s}^{-2}$. The color shading indicates the composite
 19 precipitation anomalies associated with each quintile.

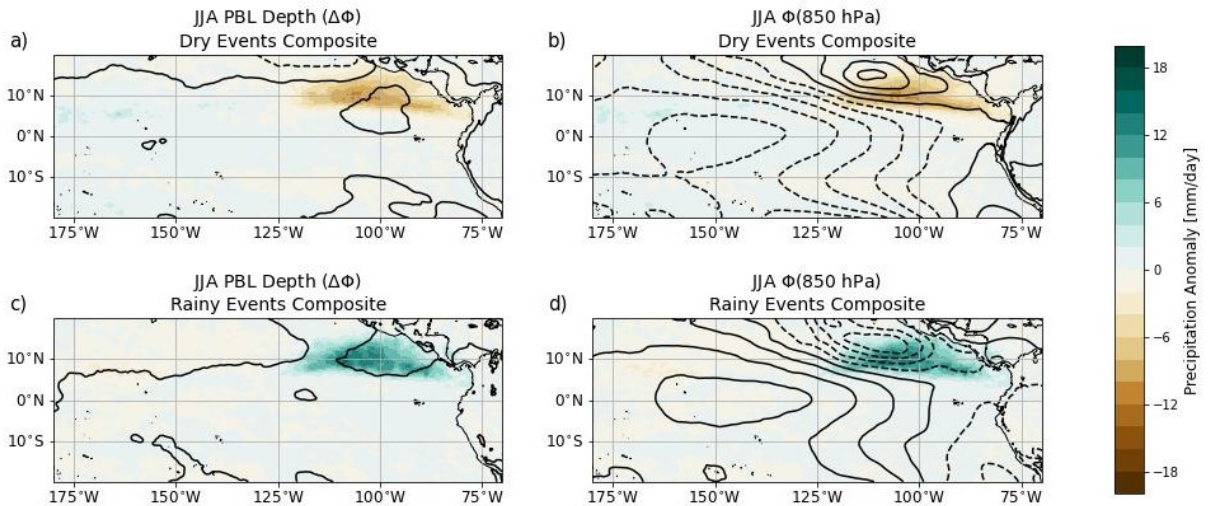
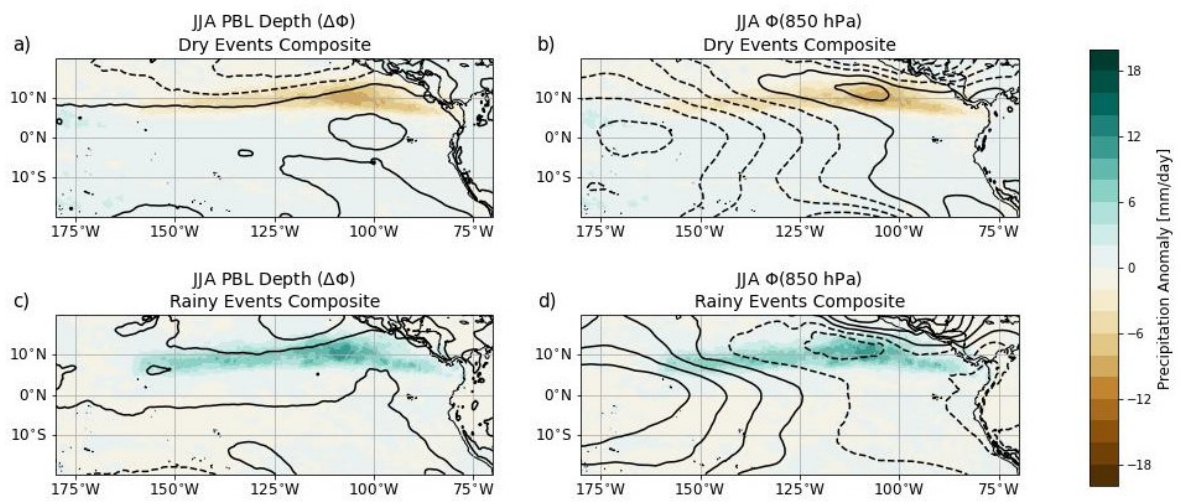
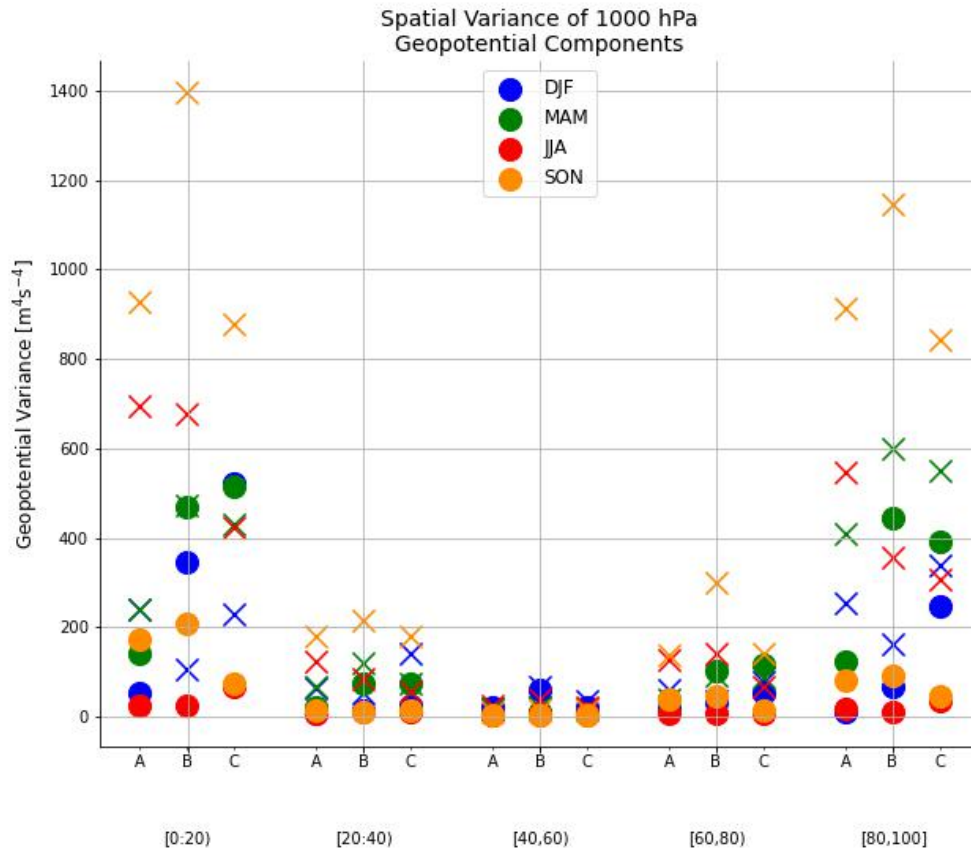


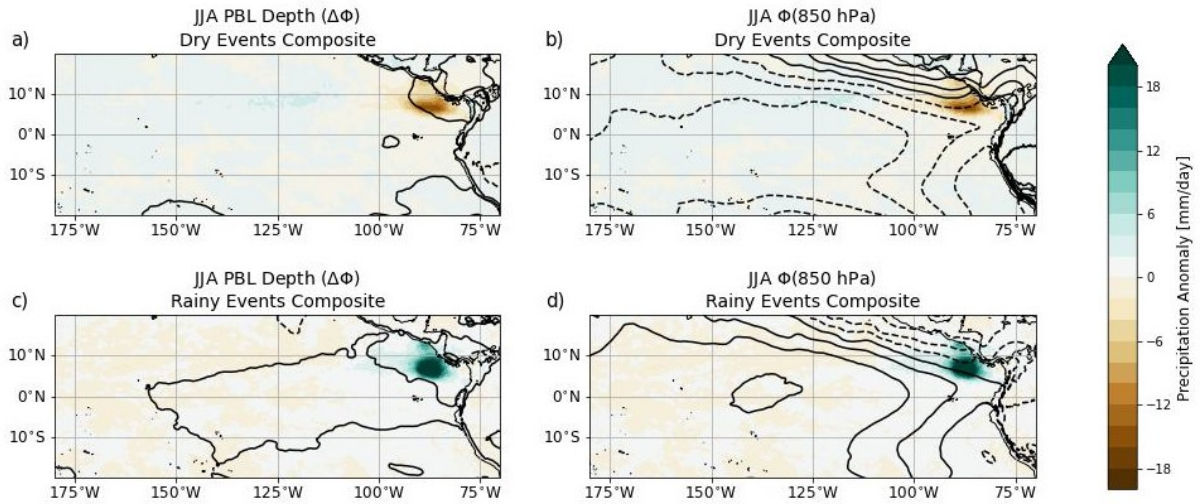
Fig. S9. As in Fig. S8, but the precipitation quintiles are now set over region B.



20 Fig. S10. As in Fig. S8, but the precipitation quintiles are now set over region C. These are the results shown
 21 in the paper.



22 Fig. S11. Spatial variance of the geopotential components for compositing done over separate regions for the
 23 daily data. The spatial variances of the PBL depth is denoted by the circle marker and the spatial variances of
 24 the 850 hPa geopotential is denoted by the x markers.



25 Fig. S12. The JJA 6-hourly averaged geopotential component anomalies composited by 6-hourly averaged
 26 precipitation quintiles over region A. Figures (a) and (c) show the PBL depth anomalies for the driest and rainiest
 27 quintiles, respectively. Figures (b) and (d) show the 850 hPa geopotential anomalies for the driest and rainiest
 28 quintiles, respectively. The contour interval for the geopotential anomalies is $10 \text{ m}^2\text{s}^{-2}$. The color shading
 29 indicates the composite precipitation anomalies associated with each quintile.

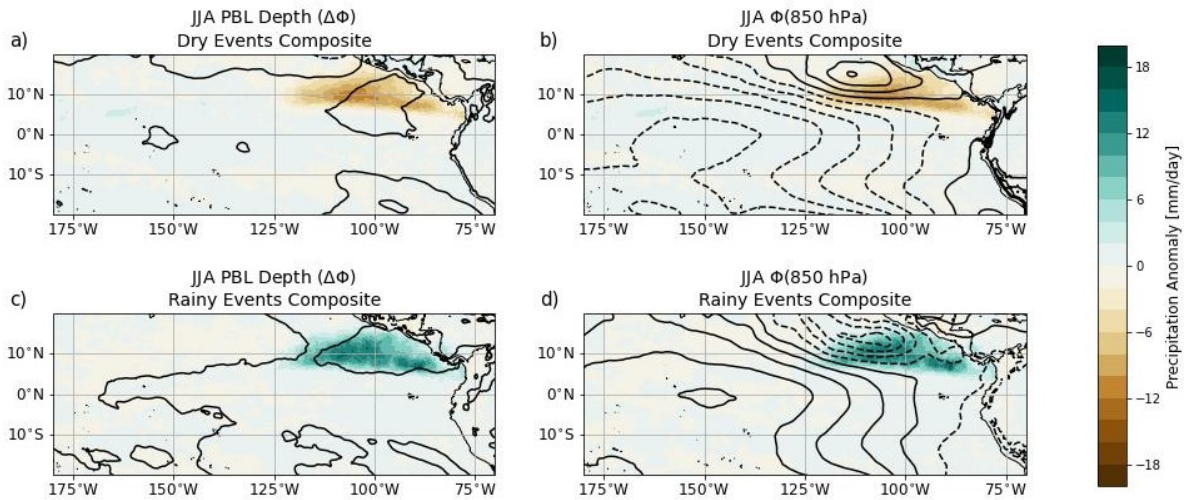


Fig. S13. As in Fig. S12, but the precipitation quintiles are now set over region B.

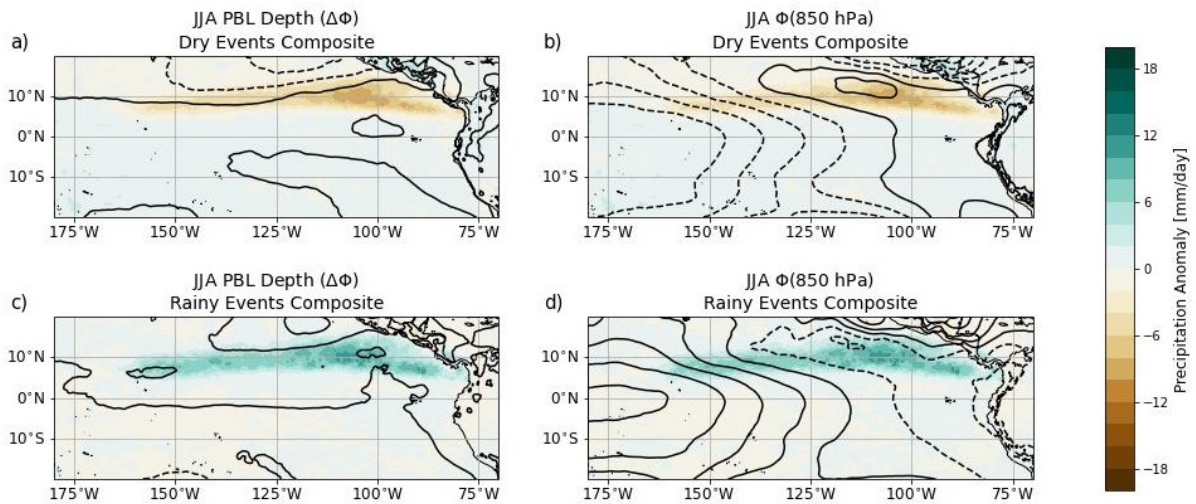
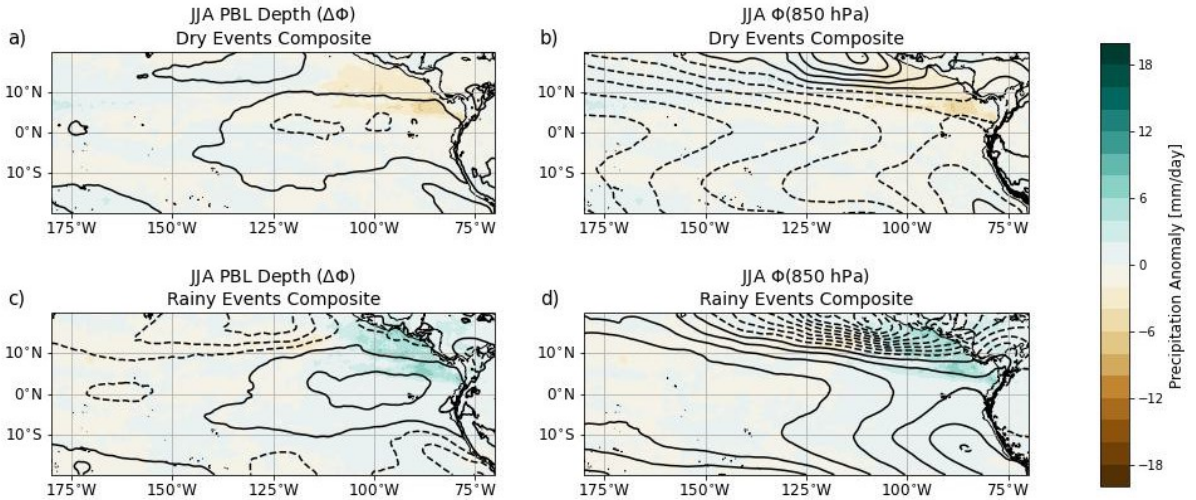


Fig. S14. As in Fig. S12, but the precipitation quintiles are now set over region C.



30 Fig. S15. The JJA 10-day averaged geopotential component anomalies composited by 10-day averaged
 31 precipitation quintiles over region A. Figures (a) and (c) show the PBL depth anomalies for the driest and rainiest
 32 quintiles, respectively. Figures (b) and (d) show the 850 hPa geopotential anomalies for the driest and rainiest
 33 quintiles, respectively. The contour interval for the geopotential anomalies is $10 \text{ m}^2\text{s}^{-2}$. The color shading
 34 indicates the composite precipitation anomalies associated with each quintile.

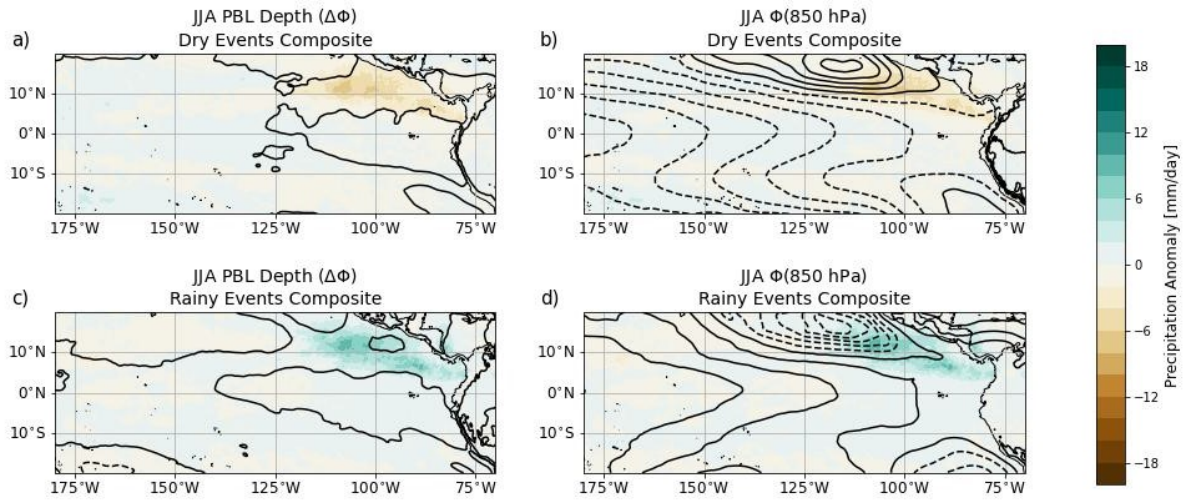


Fig. S16. As in Fig. S15, but the precipitation quintiles are now set over region B.

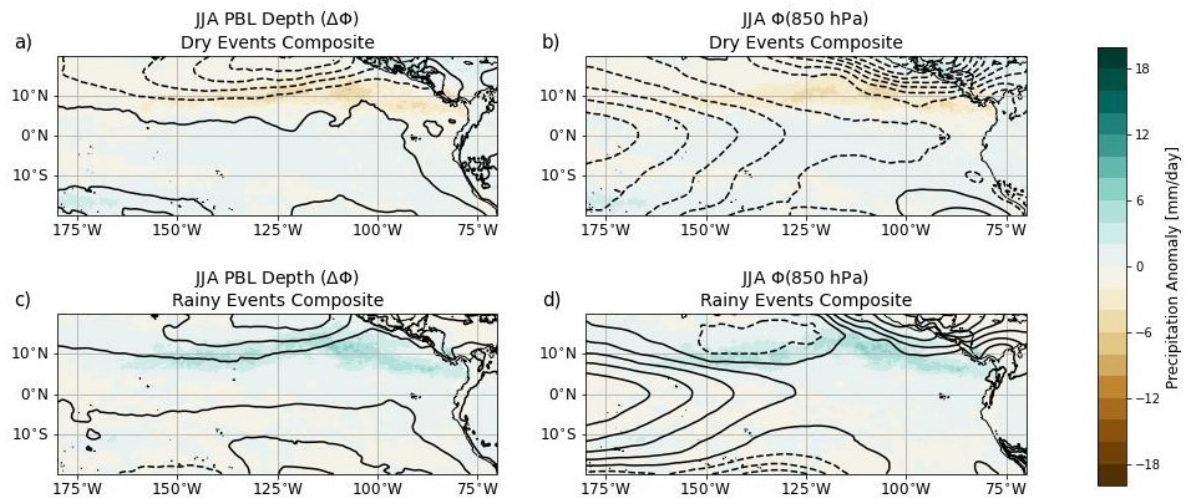
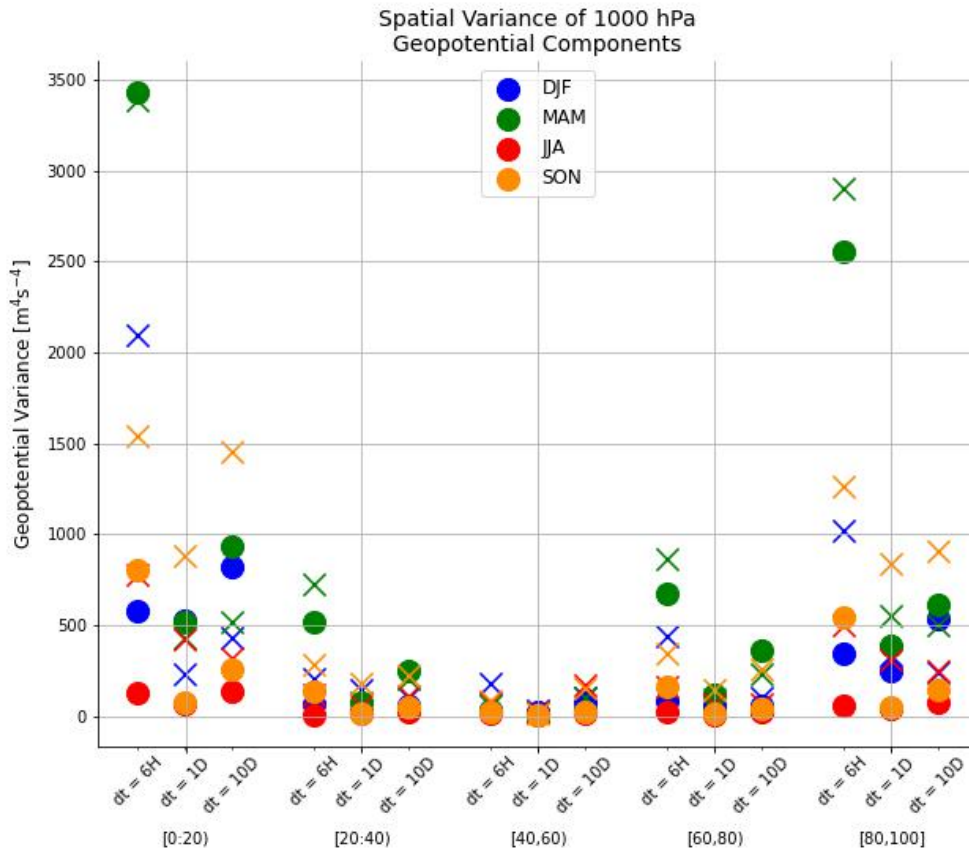


Fig. S17. As in Fig. S15, but the precipitation quintiles are now set over region C.



35 Fig. S18. Spatial variance of the seasonal geopotential components for compositing done over region C for
 36 the 6-hourly, 1-day, and 10-day averaged data. The spatial variances of the PBL depth is denoted by the circle
 37 marker and the spatial variances of the 850 hPa geopotential is denoted by the x markers.